Retrieval of Ocean Surface Wave Fields using Marine Radar-Image Sequences

Heiko Dankert and Wolfgang Rosenthal

GKSS Research Center, Max-Planck-Str. 1, 21502 Geesthacht, Germany, Email: dankert@gkss.de

***Abstract*— This paper describes and validates an empirical method for inversion of marine radar-image sequences to time series of ocean surface wave fields without calibration. External sensors are not required. The radar system can measure as a stand-alone device. The method has been developed within the framework of the European project ”MaxWave” and is based on a local description of the RCS in space and time, whereby the ocean surface is subdivided into local facets. A local transfer function between local RCS and ocean surface is determined for each facet. The inversion scheme is applied to radar-image sequences acquired by a marine X-band radar, operating at grazing incidence and horizontal polarization in transmit and receive. The system is mounted aboard an offshore platform in the North Sea. The ocean-surface image sequences are validated by comparison of the calculated significant wave heights with values from co-located wave records of three in-situ sensors. It is shown that the accuracy of the radar-retrieved significant wave height is within the accuracy of the in-situ sensors.**

I. Introduction

Ocean surface elevation fields are determined spatially and temporally from marine radar-image sequences. Thereby a novel, recently introduced, empirical method is applied and validated [1]. In-situ measurements are not required and an external calibration is not necessary. The method is very robust and assumes the main modulation of the RCS comes from the local surface slope in antenna look direction (tilt modulation). Hydrodynamic modulation is neglected, and the geometrical effect of shadowing is assumed to have a minor contribution to the RCS. The method performs well even if the relation between tilt and RCS is nonlinear.

Radar-image sequences of the sea surface are also used to measure high-resolution ocean wind fields [2], [3], wave groups [4], current fields and bathymetry in inhomogeneous areas like coastal zones or areas with current gradients [5]. Further radar images are operationally measuring two-dimensional wave-spectra and significant wave heights [6], and the mean near surface current [7].

The long ocean waves are imaged by a marine radar, because they modulate the radar backscatter from the wind-driven rough sea surface. The method is based on the determination of the surface tilt angle in antenna look direction at each pixel of the radar images. The mean radar cross section (RCS) depends on the mean local depression angle. This dependency is parameterized as a look-up table. The deviation of the RCS from the mean RCS represents a local and temporal change of the depression angle, which is assumed to be equal to the local ocean surface tilt. The translation of the RCS to the local surface tilt is a local, spatial and temporal description of the modulation process. Up to now, the modulation processes were described in the Fourier domain.

The investigations presented in this study were performed with radar-image sequences collected by a radar system installed aboard a platform in the Norwegian oil field Ekofisk in the central North sea using the Wave Monitoring System (WaMoS), which has been developed at GKSS Research Center. The sensor is a conventional marine radar, operating at X-band (9.5 GHz) with horizonal (HH) polarization in transmit and receive. The radar technique allows the spatial-temporal measurement of the backscatter from the ocean surface under most weather conditions, independent of light conditions [8].

For validation the method has been applied to more than 1500 data sets from Ekofisk. Co-located measurements from three in-situ sensors, one wave rider buoy and two laser sensors, were taken. Thereby a comparison of the significant wave height from the inverted radar-image sequences and the co-located in-situ data was performed. The results show the robustness of the inversion method.

II. Investigated data

All investigated data have been recorded in the ConocoPhillips operated Ekofisk oil field in the North Sea from the platform ”2/4k” (56.5°N, 3.2°E, cf. Fig. 1). The water depth in this area is about 70 m. All radar-data sets were taken by WaMoS II, that enables the continuous digitization of radar-image sequences. The sensor, a marine radar, installed 74 m above mean sea level, operates at 9.5 GHz (X-band) with HH polarization near grazing incidence. It covers an area within a radius of $\approx$ 2000 m with a resolution of $\approx$ 12 m in range. The radar antenna rotates with period 2 s. A standard radar-data set consists of 32 images representing $\approx$ 82 s. The investigated radar-image sequences and co-located in-situ data, provided by one wave-rider buoy and two laser sensors (see Fig. 1), cover 8 months, from February until September 2001. They represent more than 1500 acquisition times with significant wave heights up to $H_S \approx 6$ m. The wind speed was up to ≈ 17 ms^{-1}. The data provided by the in-situ sensors are continuous measurements of the sea surface elevation, whereas the sea state parameters are determined for time intervals of 20 minutes. The sampling frequency is 2 Hz.

III. Ocean Surface Determination

A. Imaging Mechanisms

Ocean waves are visible by a real aperture radar, like a marine radar, due to modulation of the RCS by the long

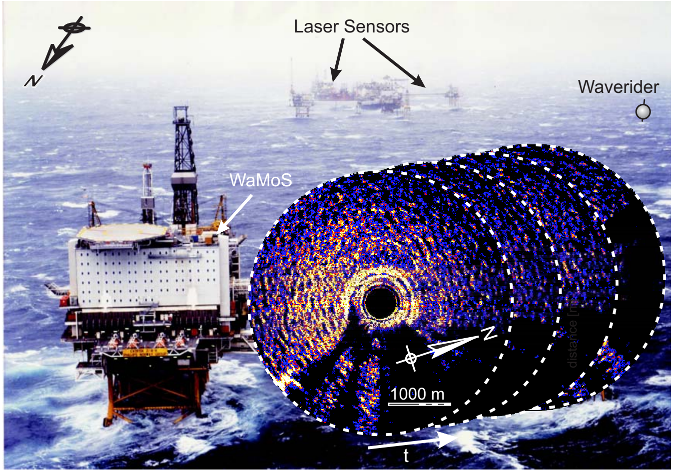

Fig. 1. WaMoS system installed on Platform "2/4k" of the Ekofisk oil field in the North Sea. A wave rider buoy is placed near the oil field, and the two laser sensors are mounted on the main complex.

surface gravity waves. This modulation of the RCS is a sum of four contributing processes: the geometrical effects of shadowing and tilt, hydrodynamic modulation, and wind modulation. For the determination of the ocean surface by the developed empirical method, it is assumed, that the RCS is mainly modulated by the wind and the ocean surface tilt:

$$M = M_{aero} + M_{tilt}. \tag{1}$$

Hydrodynamic modulation is neglected here. Shadowing appears only in the very far range at Ekofisk, because of the given antenna height (74 m), and is therefore assumed to have a minor contribution to the RCS.

Mathematically the modulation process is described by a modulation transfer function (MTF), which is commonly defined as expansion of the RCS for the spectral amplitudes of the wave field $\hat{\eta}(\vec{k})$ [9]. For a local facet at location $\vec{r}$ and time t the local RCS is given by [1]:

$$\begin{aligned}\sigma_0(\vec{r},t) &= \overline{\sigma}_0(\vec{r},t) + \delta\sigma_0(\vec{r},t) \\ &= \overline{\sigma}_0(\vec{r},t) \cdot \left(1 + M(\vec{\vec{k}}|\vec{r},t) \cdot \underbrace{e^{i\vec{\vec{k}}\cdot\vec{r}} \cdot A(\vec{r},t)}_{\eta(\vec{r},t)}\right) \end{aligned} \tag{2}$$

describing the deviation of the RCS $\delta\sigma_0$ at location $\vec{r}$ and time t as a product of the local modulation function $M(\vec{\vec{k}}|\vec{r},t)$ and the local wave field $\eta(\vec{r},t)$ as indicated in (2). Thereby the local wave field is a product of a carrier wave with wave number $\vec{\vec{k}}$ and a slowly varying amplitude function $A(\vec{r},t)$. This translation of the RCS to the local surface tilt is a local, spatial and temporal description of the modulation process. The MTF is therefore a spatial and temporal function, which has to be determined for each location. This is different from the description of the MTF in the spectral domain.

The inversion method is based on this local, spatial and temporal description of the modulation process by determination of the surface tilt angle in antenna look direction at each pixel of the radar-image sequences. The mean RCS is dependent on the local depression angle at X-band and HH polarization [10]. This (linear or non-linear) dependency is parameterized as a look-up table. The deviation of the RCS from the mean RCS represents a local temporal change of the depression angle, which is assumed to be equal to the local ocean surface tilt.

B. Method

The inversion scheme in Fig. 2 gives an overview of the method for determination of time series of ocean surface elevation maps. The input for the method are the raw polar radar-image sequences $\sigma_0(\vec{r},t)$ as shown in Fig. 1.

Real aperture antennas are directional antennas, which radiate radio-frequency energy in patterns of lobes that extend outward from the radar antenna in antenna look direction. The radiation pattern also contains minor lobes. Because of the radiation pattern, each radar antenna has a typical receiving pattern. An important step to analyze the radar images is to know this receiving pattern and to correct the data. Therefore, in a first step, each radar image is corrected with the characteristic antenna receiving pattern. For details regarding the measuring of the antenna receiving pattern refer to [1].

In the next step the dependency between the local variation of the RCS σ_0 from the mean RCS $\overline{\sigma}_0$ and the local tilt φ has to be determined. The mean RCS is dependent on the local depression angle Ψ at X-band and HH polarization [10]. The deviation of the RCS $\delta\sigma_0$ from the mean RCS $\overline{\sigma}_0$ represents a local and temporal change of the depression angle, which is assumed to be equal to the local ocean surface tilt. The mean RCS is parameterized for each antenna-look direction ϕ_i:

$$\tilde{\sigma}_{0,i}(r,\phi_i) = f(r,\phi_i), \tag{3}$$

where $f(r,\phi_i)$ gives the parametrization function and $\tilde{\sigma}_0$ the resulting 2-D parametrization. The range-dependent depres-

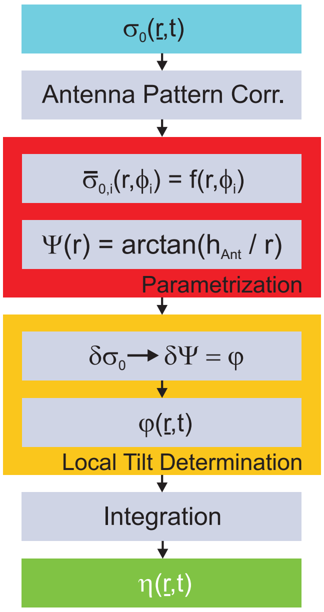

Fig. 2. Inversion scheme for determination of ocean surface elevation.

sion angle $\tilde{\Psi}$ is given by:

$$\tilde{\Psi}(r) = \arctan(h_{ant}/r), \tag{4}$$

with r giving the distance from the antenna and the given installation height of the radar antenna $h_{ant} = 74$ m.

The ocean surface waves cause a local change of the depression angle $\delta\Psi$, the tilt modulation of the RCS, and thereby a local deviation of the RCS $\delta\sigma_0$ from the mean value $\overline{\sigma}_0$. With the given parameterizations (3), (4) and the known deviation of the RCS $\delta\sigma_0$ from its mean value, the local change of the depression angle $\delta\Psi$ is determined, which is assumed to be equal to the local ocean surface tilt φ (see Fig. 2). The local tilt angles are determined for each location in space and time. The result is a sequence of tilt images $\Phi(\vec{r}, t)$. For details refer to [1].

The ocean surface elevation $\eta(\vec{r}, t)$ is determined from the tilt angles $\Phi(\vec{r}, t)$ directly by integration. Thereby tilt-image sequence $\Phi(\vec{r}, t)$ is transformed into the wave-number frequency domain by performing a 3-D Fast-Fourier Transform (FFT). The resulting complex 3-D tilt spectrum $\hat{\Phi}(\vec{k}, \omega)$ is integrated by multiplying with an integration transfer function $\hat{D}$, that is complex and shifts the phase of all wave number components in the Fourier space by $\pi/2$.:

$$\hat{\eta}(\vec{k}, \omega) = \hat{\Phi}(\vec{k}, \omega) \cdot \hat{D}. \tag{5}$$

The result is a complex 3-D wave spectrum $\hat{\eta}$ of the ocean surface elevation field.

The integration process causes an amplification of small wave numbers. Therefore a posterior filtering process is necessary to retrieve only the signal of the ocean surface wave field. The dispersion relation of linear surface-gravity waves is used, that connects wave numbers k with their corresponding frequency coordinates ω [8]:

$$\varpi = \sqrt{gk \tanh kd} + \vec{k} \cdot \vec{u} \tag{6}$$

where ϖ indicates the absolute frequency, g the gravitational acceleration, d the water depth, and $\vec{u}$ the velocity of encounter. The filtering is done by fitting the theoretical dispersion relation to the signal coordinates in the complex wave-number frequency spectrum [7]. Thereby the dispersion shell is strongly broadened in k and ω to get also components of the wave spectrum that do not lie exactly on this function. To suppress those Fourier coefficients with small wave numbers and those with noise from non-relevant spectral components additionally a bandpass filter is applied (cf. [1]). The wave field $\eta(\vec{r}, t)$ is determined by transforming the retrieved complex 3-D wave spectrum $\hat{\eta}_W(\vec{k}, \omega)$ into the spatial-temporal domain by an inverse 3-D FFT.

Fig. 3 shows a resulting ocean-surface elevation image sequence, recorded on March 28th, 2001 at Ekofisk 2/4k. An azimuthal dependency of the ocean surface elevation is clearly visible. This dependency is explained as a geometrical projection factor as follows: only the tilt component of the water surface in the antenna viewing direction affects the modulation of the RCS. Therefore the RCS is not modulated if the radar is looking parallel to the wave crests. The significant wave height in the area around the given wave travel direction for the whole image sequences is $H_S = 4.47$ m, which is in excellent agreement with $H_S = 4.47$ m, retrieved from a co-located buoy-time series.

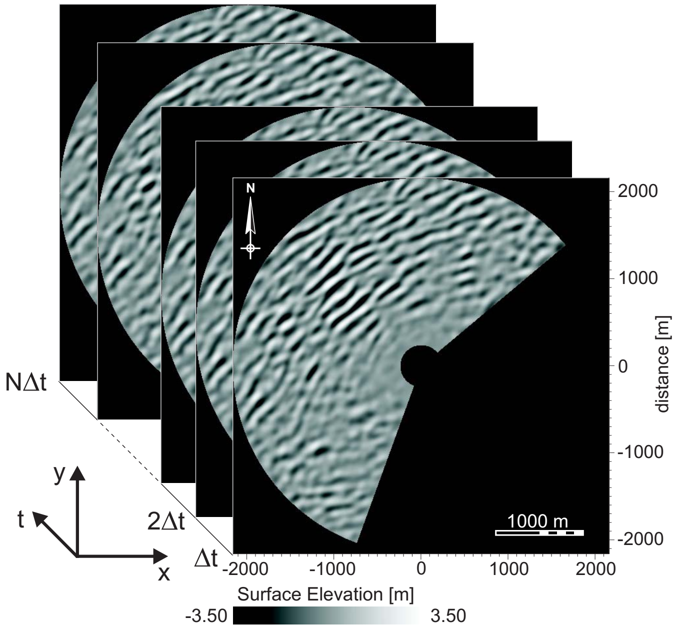

Fig. 3. Ocean surface elevation sequence of a radar-image sequence recorded on March 28th, 2001 at Ekofisk 2/4k (see Fig. 1). The determined H_S is 4.47 m compared to 4.47 m retrieved from a co-located time series of the wave rider buoy.

IV. Validation

This section is focused on the statistical comparison of the ocean-surface elevation image sequences with the co-located 2 Hz elevation time series (20 minutes each) of three in-situ sensors, one wave rider buoy and two laser sensors (”Flare North” (FN) and ”Flare South” (FS)). All in-situ sensors are situated within the radar measuring range.

The comparison is focused on the significant wave height H_S as integral statistical parameter, the most important quantity used describing a sea state. H_S is directly determined from the standard deviation of the spatial-temporal wave elevation:

$$H_S = 4 \cdot \left\langle (\eta(r, \phi, t) - \overline{\eta})^2 \right\rangle^{\frac{1}{2}}, \tag{7}$$

where $\overline{\eta}$ gives the population mean, and $\langle \cdot \rangle$ denotes the expectation value of η. H_S is determined only for the area within $\pm 22.5°$ of the wave travel direction $\phi_W \pm 180°$, due to the radar is mainly imaging waves which travel towards and away from the radar. For the in-situ time series H_S is also directly determined from the standard deviation of the elevation-time series.

1535 radar data sets with H_S up to 6 m are processed, together with their co-located time series from the in-situ sensors. Only data sets, recorded under a minimum wind speed conditions of ≈ 4 ms^{-1} are considered. This wind speed is necessary for a measurable modulation of the RCS.

Fig. 4a gives exemplary a comparison of H_S between wave-rider buoy and marine radar, and Fig. 4b between buoy and laser FN. In both cases a correlation of 0.93 and a standard

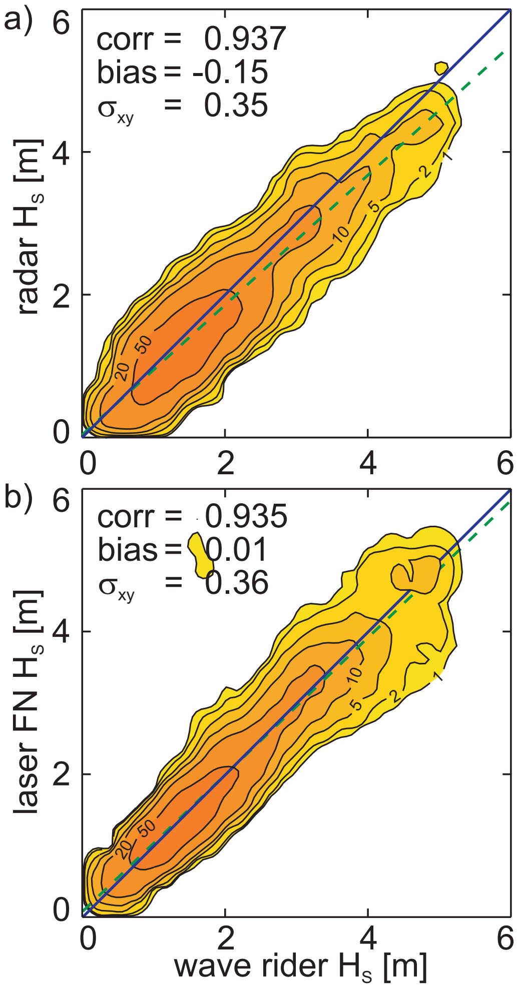

Fig. 4. Comparison of H_S derived from 1535 wave-rider records with radar-H_S values (a), and with H_S derived from wave records of laser FN.

deviation of 0.35 m could be achieved. With a bias of 15 cm the radar is slightly underestimating the measurements of the buoy. Table I shows a full inter-comparison between all 4 sensors. Thereby the upper three rows give the comparison between the radar measurements and those from the in-situ sensors. The lower three rows of Table I give an inter-comparison between all three in-situ sensors. Correlation, bias and standard deviation between the in-situ sensors are within the same range as between the in-situ sensors and the radar. Different from the buoy, the bias between radar and laser FS is neglectible. It is obviously that the accuracy of the in-situ sensors is decreasing with increasing wave height. For the radar measurements it is nearly constant (cf. Fig. 4).

sensor 1	sensor 2	corr	bias	σ_{xy}
radar	wave rider	0.94	0.15	0.35
radar	laser FN	0.90	0.17	0.44
radar	laser FS	0.90	0.03	0.43
wave rider	laser FN	0.93	0.01	0.36
wave rider	laser FS	0.96	-0.12	0.27
laser FN	laser FS	0.90	-0.14	0.43

TABLE I

MAIN STATISTICAL PARAMETERS RESULTING FROM COMPARISON OF 1535 H_S VALUES BETWEEN TWO DIFFERENT SENSORS.

V. CONCLUSIONS

An recently introduced empirical inversion scheme has been applied and validated [1]. This has been done by comparison to in-situ wave measurements considering a data set of more than 1500 radar-image sequences with co-located in-situ measurements with significant wave heights H_S up to 6 m. The method is based on the determination of the tilt angle of the ocean surface at each pixel of the radar images. The modulation of the RCS by the ocean surface tilt is described locally, spatially and temporally. A calibration procedure is not necessary. The radar system can measure as a stand-alone device. H_S has been determined from the radar-derived time series of ocean surface elevation maps and compared to significant wave heights from co-located in-situ wave records. Comparison resulted in a correlation of 0.93 and a standard deviation of 0.35 m. An inter-comparison between all four sensors was performed. Correlation, bias and standard deviation are within the same range for all sensors.

ACKNOWLEDGMENTS

The authors were supported by the European Commission in the framework of the EU project MaxWave. All radar-image sequences were kindly made available by the company OceanWaves.

REFERENCES

[1] H. Dankert and W. Rosenthal, “Ocean surface determination from x-band radar-image sequences,” *J. Geophys. Res.*, vol. 109, no. C04016, doi: 10.1029/2003JC002130, 2004.

[2] H. Dankert, J. Horstmann, and W. Rosenthal, “Ocean wind fields retrieved from radar-image sequences,” *J. Geophys. Res.*, vol. 108, no. C11, 3352, doi: 10.1029/2003JC002056, 2003.

[3] H. Dankert, J. Horstmann, and W. Rosenthal, “Ocean surface winds retrieved from marine radar-image sequences,” *Proc. Int. Geosci. Remote Sens. Symp.*, 2004.

[4] H. Dankert, J. Horstmann, S. Lehner, and W. Rosenthal, “Detection of wave groups in SAR images and radar-image sequences,” *IEEE Trans. Geosci. Remote Sens.*, vol. 41, no. 6, pp. 1 437–1 446, 2003.

[5] H. Dankert, “Retrieval of surface-current fields and bathymetries using radar-image sequences,” *Proc. Int. Geosci. Remote Sens. Symp.*, 2003.

[6] J.C. Nieto Borge, K. Hessner, and K. Reichert, “Estimation of the significant wave height with x-band nautical radars,” in *Proc. 18th Intern. Conf. on Offshore Mech. and Arctic Eng. (OMAE)*, St. John's, Newfoundland, Canada, 1999, number OMAE99/OSU-3063.

[7] C.M. Senet, J. Seemann, and F. Ziemer, “The near-surface current velocity determined from image sequences of the sea surface,” *IEEE Trans. Geosci. Remote Sens.*, vol. 39, pp. 492–505, 2001.

[8] I.R. Young, W. Rosenthal, and F. Ziemer, “A threedimensional analysis of marine radar images for the determination of ocean wave directionality and surf. curr.,” *J. Geophys. Res.*, vol. 90,C1, pp. 1049–1059, 1985.

[9] W. R. Alpers, D. B. Ross, and C. L. Rufenach, “On the detectability of ocean surface waves by real and synthetic aperture radar,” *J. Geophys. Res.*, vol. 86, pp. 6 481–6 498, 1981.

[10] D.B. Trizna and D.J. Carlson, “Studies of dual polarized low grazing angle radar sea scatter in nearshore regions,” *IEEE Trans. Geosc. Remote Sens.*, vol. 34, pp. 747–757, 1996.